First Result of the SMA Holography Experirnent

Xiaolei Zhang
Peter Bratko
Dan Oberlander
Nimesh Pate1
Tirupati K. Sridharan
Antony A. Stark

December 11, 1996

Submillimeter Array Memorandum, No. 102

Abstract

This memo summarizes the result of the first holography run, which obtained a 6-l by 64 beam map of the SMA antenna 1. After Fourier transform and large scale error fitting, the aperture phase map revealed a dish surface with rms error about 130 micron. Subsequent panel fitting and the removal of fitted panel errors result in a residual surface rms error about 14 micron if including the quadrupod shadow region, and 5-10 micron if not.

The First Beam Map

The first beam map of the SMA antenna 1 was taken on December 3. 1996, using the newly-installed holography data acquisition system (Zhang et al. 1995), which consists of two room temperature phase-locked receivers, and a phase-locked beacon transmitter located on a tower 250 meters away. The gain stability of the holography data acquisition system is better than 1%, and the short-term phase stability is about a fraction of a degree. A vector-voltmeter backend is used for detection. and the post-detection signal to noise ratio is about 100 dB at the boresight direction.

Figure 1 shows the image of the first measured beam pattern (amplitude only. Phase pattern was taken simultaneously but not shown here). Since at the time of this measurement: the boresight coordinates were not accurately determined (the program we used to measure this pattern is actually meant to assist the determination of the boresight direction), the beam is seen to be slightly off-centered. 'The overall pattern, however, is consistent with what is expected of an antenna focused towards 250 meter distance. The signature of the SMA quadrupod structure, a pattern rotated '7.3 degrees clockwise from vertical and horizontal symmetry, can also be discerned.

Due to the lack of an accurate boresight direction, gain and phase calibration ad the boresight is not made during the mapping. Our experience so far with the data acquisition system, however, shows that the temporal drift of amplitude and phase levels is minimal. This 64 by 64 map took about one hour and 10 minutes to acquire. It is expected that in the near future, we will be able to optimize the data acquisition software so that a 128 by 128 map can be acquired within an hour.

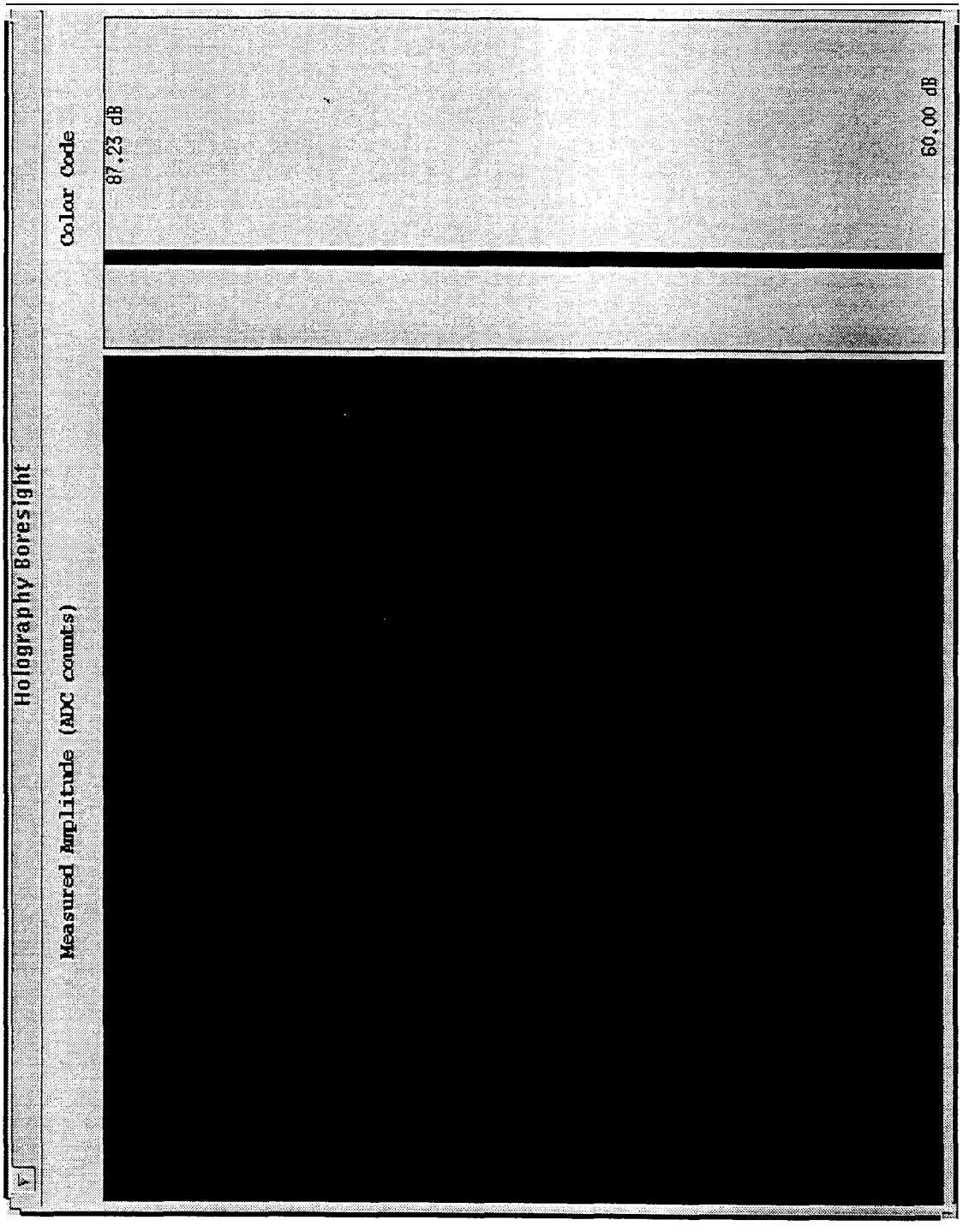

Figure 1: Measured beam pattern of the SMA antenna 1.

Analysis

The measured amplitude and phase patterns were then input to the analysis package HOLIS (Zhang 1996) for processing. After the preprocessing stage to move the phase reference plane to that in the middle of the dish, and after a subsequent Fourier transform, we obtain the amplitude and phase distributions of the electric field on the antenna aperture: as shown in Figures 2 and 3. Note that since we have a large pointing offset to the boresight direction, the linear phase gradient on the aperture is very large. The phase in fact has wrapped around 2π a couple times, and we unwrapped the phase to arrive at the phase distribution shown in Figure 3.

In Figure 2, the amplitude suppression at the location of the quadrupod is clearly seen. A blanking of the region inside the subreflector and outside the dish, however. was artificially made. Although a linear phase gradient dominates the phase map of Figure 3, some large ring-like ripples are seen on the phase map, indicating the presence of the secondary mirror diffraction contribution (Zhang 1995) to the phase pattern.

After taking out six terms of large-scale errors (constant term, x and y linear gradient, defocus: diffraction, as well as the distance uncertainly to the transmitter), we obtain a residual map of the small-scale phase errors. caused mainly by the mis-alignment of the panels from a perfect paraboloid. Converting the phase error map to a surface error map (Zhang 1995), we then obtain the distribution shown in Figure 4.

From Figure 4, we see that the maximum surface error is about 500 micron, and the calculated surface rms error is about 130 micron. The location of the quadrupod, the separation between the different rings of panels, as well as a few very-badly misplaced panels can also be discerned in Figure 4. The relatively large amount of surface error near the area where the quadrupod legs connect to the outer dish is likely to be due to that, during the assembly phase, the dish was lifted up at these locations and thus has deformed accordingly. The slight asymmetry between the widths of the panel-sized structures in the left and right hand side of the dish, is due to that the center of the dish is located on cell (33,33) in this 64 by 64 map, so there is expected to be a maximum one-cell difference in the size of structures in the left and right. This artifact will be reduced in a 128 by 128 map.

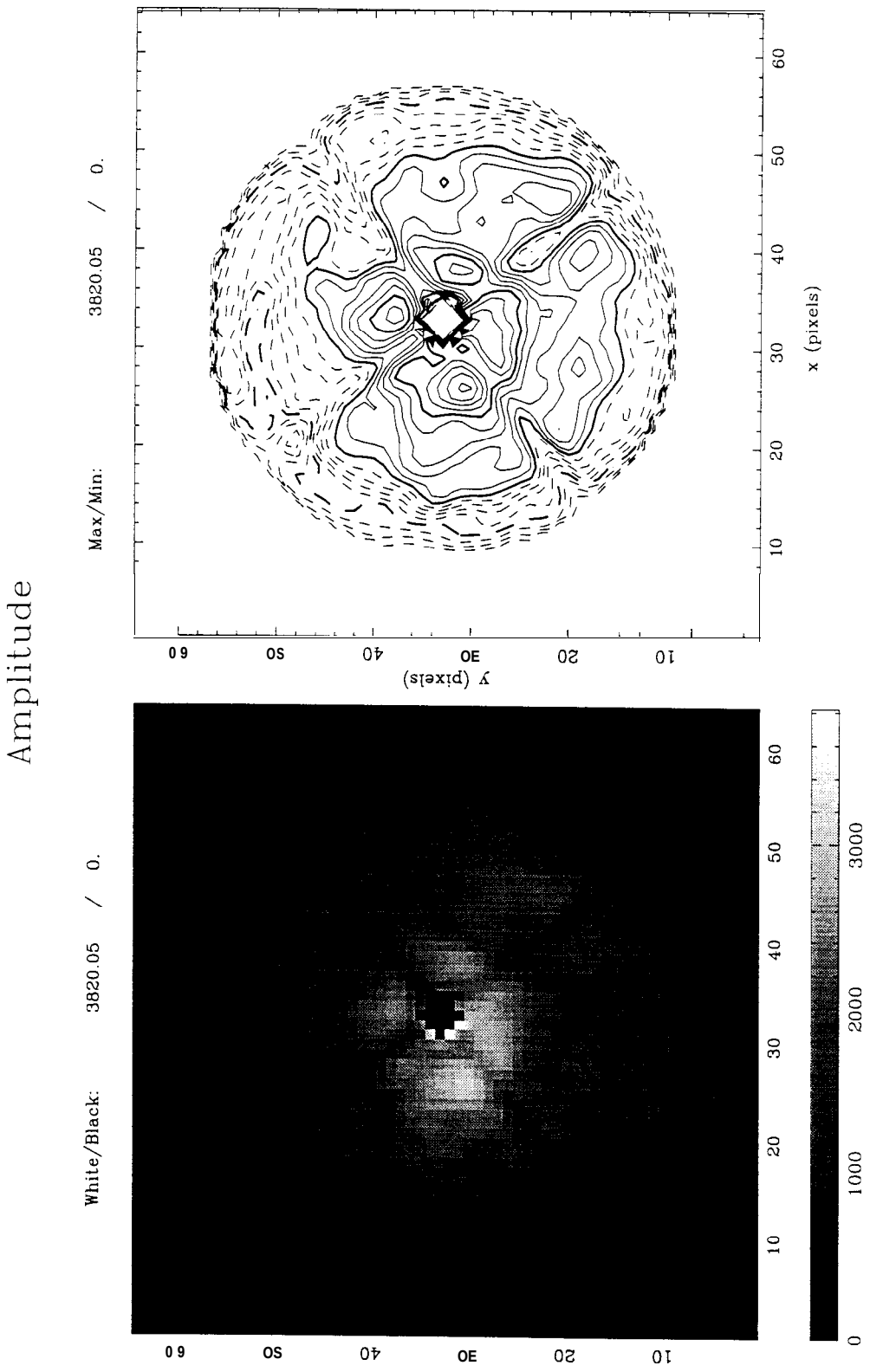

Figure 2: Amplitude pattern on the antenna aperture.

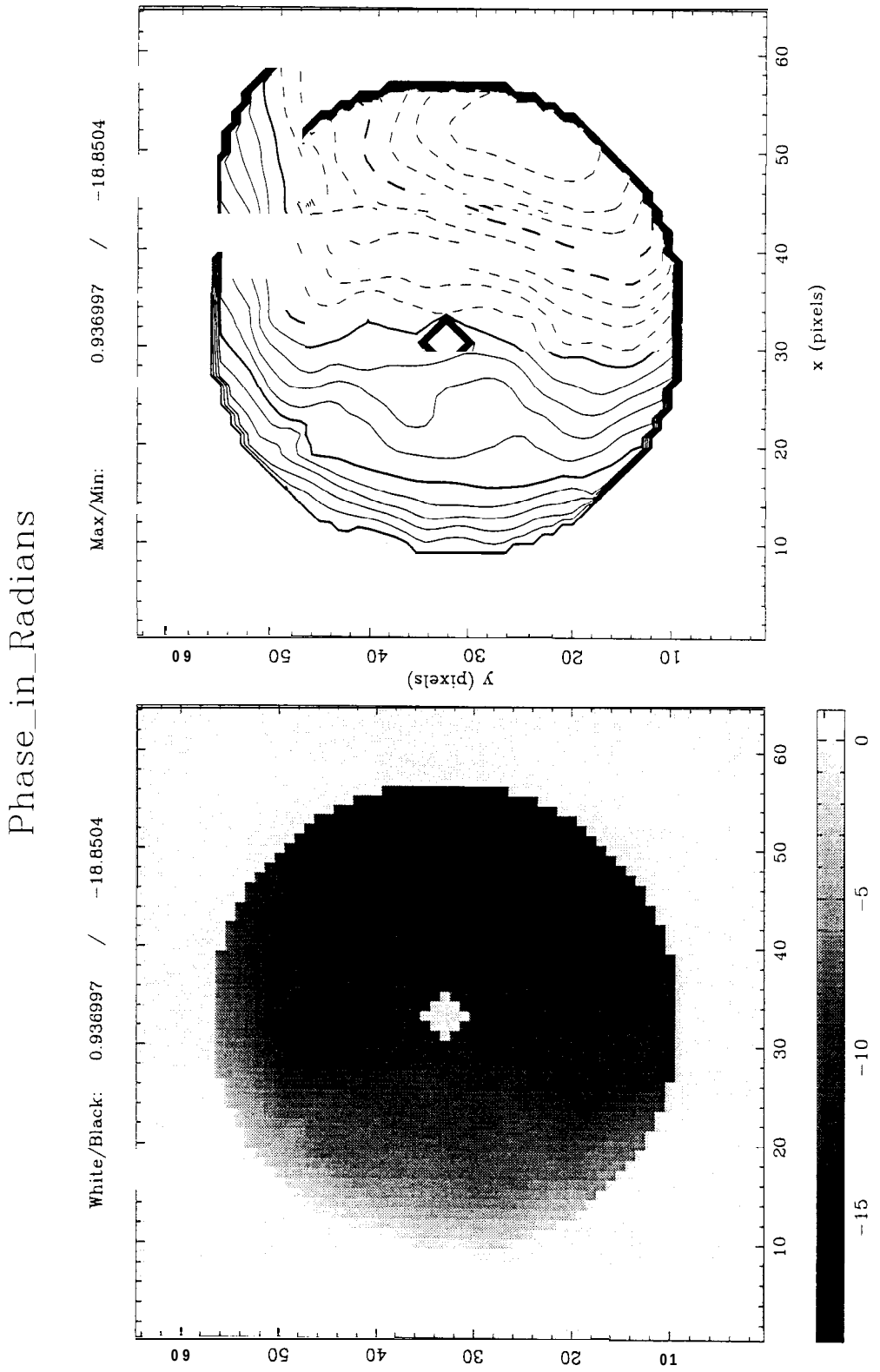

Figure 3: Phase distribution on the antenna aperture, after unwrapping a 2π ambiguity.

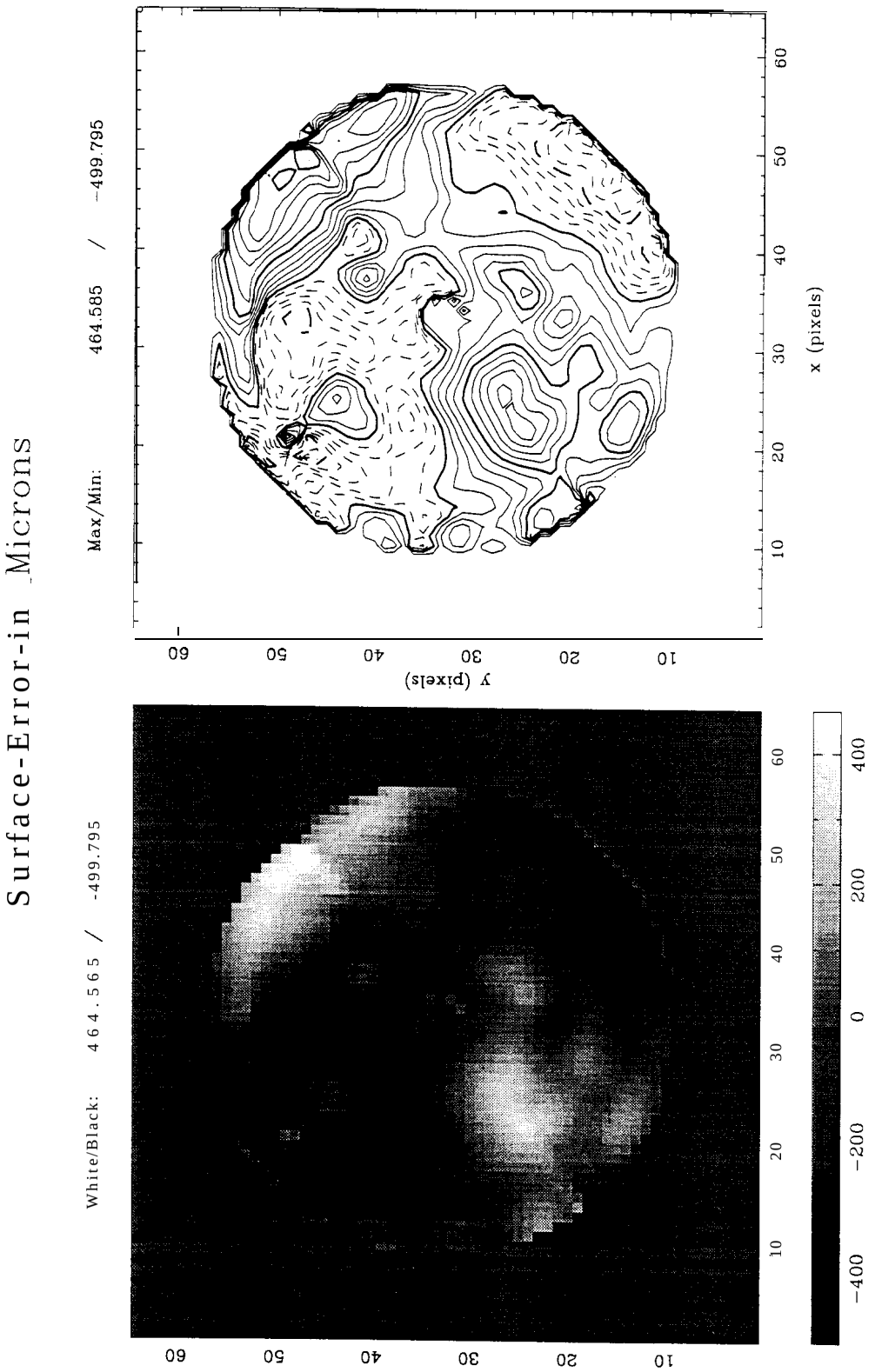

Figure 4: Surface error distribution on the aperture after taking out the large-scale error terms. The rms surface error is 130 micron.

Fitting the Individual Panel Movement

The phase error map of Figure 4 is subsequently used by the panel-fitting routines in HOLIS to calculate the screw motions needed on each panel to reduce the surface error. The residual error map after panel fitting is shown in Figure 5. Here we see the dominance of the quadrupod pattern as well as its shadow in the outer dish. The ripples in the outer ring is expected to be the aliasing effect produced by the quadrupod shadow. This latter effect is expected to be reduced once a 128 by 128 map is made. The residual surface rms error after the panel fitting is about 14 micron. If we ignore the quadrupod shadow region, the residual rms is between 5-10 micron.

Summary

The first SMA holography test run successfully measured the beam pattern on antenna 1. The aperture phase distribution obtained from this beam pattern clearly indicates the four rings of SMA panels, as well as the signature of individual panel misalignments. The next phase of holography effort will concentrate on improving the speed of the data acquisition, verifying the repeatability of the measurement, understanding the possible source and correction of systematic errors, as well as improving the alignment of the various components in the optical path. Actual panel adjustments will begin when a high-resolution (128 by 128), repeatable aperture phase map is made, in the near future.

Acknowledgement

We thank the SMA staff at the Haystack construction site, at the Cambridge site, as well as at the submillimeter wave receiver lab for helpful assistance. Martin Levine;. John Test and Cosmo Papa were involved in the first stage of the hardware preparation. Colin Masson and Bob Wilson provided useful technical advice. We thank Jim Moran, Eric Silverberg and Bill Bruckman for management assistance in making the first holography run happen in a timely fashion.

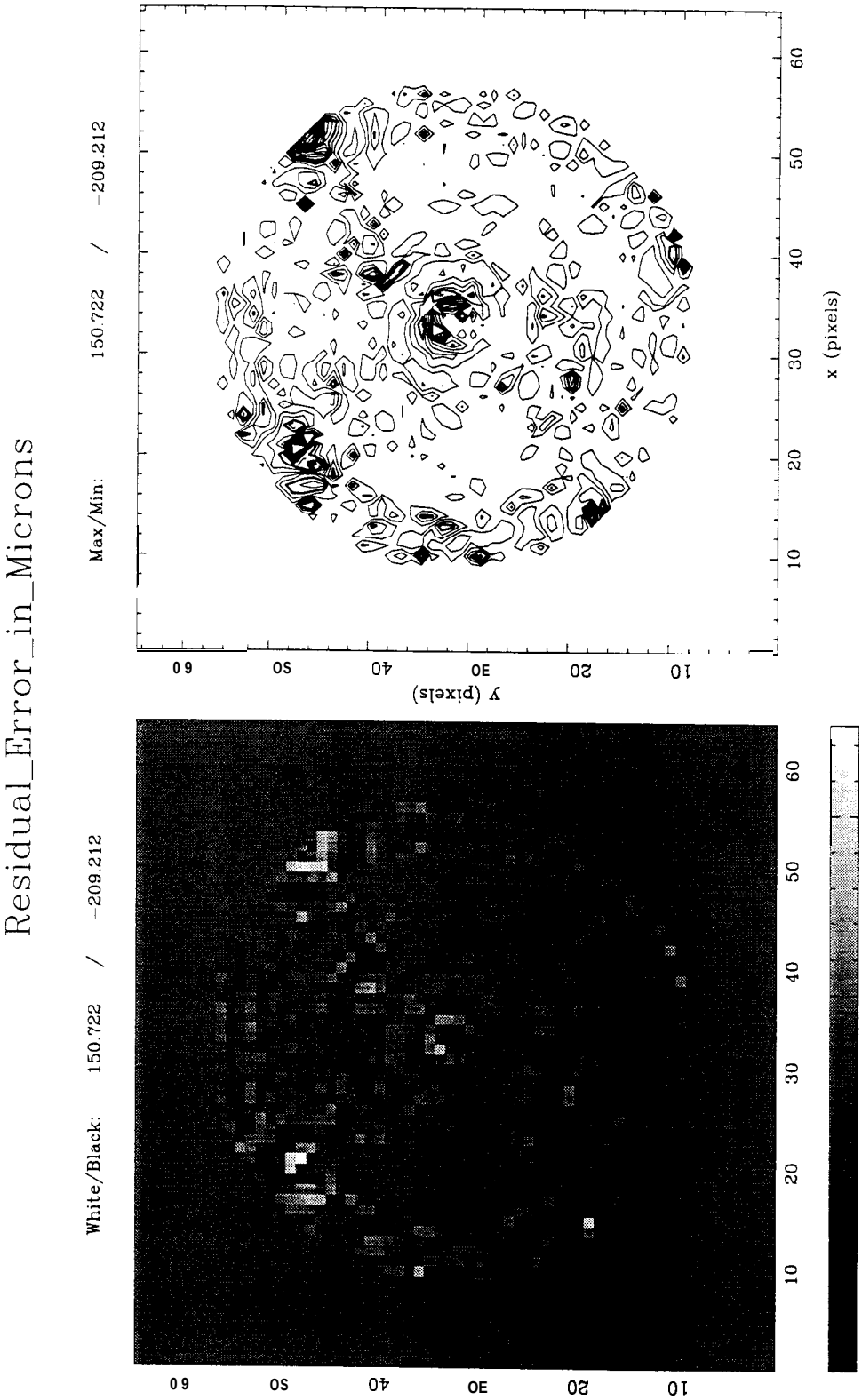

Figure 5: Residual error distribution on the aperture after panel fitting. The rms surface error is 14 micron.

References

Zhang, X. 1996, "HOLIS User's Manual," in preparation.

Zhang, X., Levine, M., Bratko, P., Test, J., Papa, C. and Masson, C. "Planned Panel Alignment Procedure for the SMA Antennas Using the Microwave Holography Technique:" SMA technical memo, No. 85

Zhang, X. 1995, "Certain Optics Considerations for the Holography Experiment," SMA Techical memo, No. 36